Pure & Appl. Chem., Vol.52, pp.1359-1386.
Pergamon Press Ltd. 1980. Printed in Great Britain.

0033-4545/80/0501-1387$02.00/0

INTERNATIONAL UNION OF PURE AND APPLIED CHEMISTRY

MACROMOLECULAR DIVISION

COMMISSION ON POLYMER CHARACTERIZATION AND PROPERTIES

WORKING PARTY ON STRUCTURE AND PROPERTIES OF COMMERCIAL POLYMERS*

A COLLABORATIVE STUDY ON THE MELT RHEOLOGY OF A STYRENE-BUTADIENE-STYRENE BLOCK COPOLYMER

Prepared for publication by
A. GHIJSELS and J. RAADSEN
Koninklijke/Shell-Laboratorium, Amsterdam

*Membership of the Working Party during the period 1974-79 in which the report was prepared was principally as follows:

Chairman: P. L. CLEGG (UK); *Secretary*: M. E. CARREGA (France); *Members*: G. AJROLDI (Italy); G. G. A. BÖHM (USA); F. N. COGSWELL (UK); M. FLEISSNER (FRG); A. GHIJSELS (Netherlands); J. HEIJBOER (Netherlands); A. S. LODGE (USA); J. MEISSNER (Switzerland); H. H. MEYER (FRG); H. MUNSTEDT (FRG); A. PLOCHOCKI (Poland); A. K. VAN DER VEGT (Netherlands); G. V. VINOGRADOV (USSR); A. J. DE VRIES (France); J. L. S. WALES (Netherlands); H. H. WINTER (FRG); J. YOUNG (Netherlands).

A COLLABORATIVE STUDY ON THE MELT RHEOLOGY OF A STYRENE-BUTADIENE-STYRENE BLOCK COPOLYMER

A.Ghijsels and J. Raadsen

Koninklijke/Shell-Laboratorium, Amsterdam
(Shell Research B.V.)
Badhuisweg 3, 1031 CM Amsterdam, The Netherlands

Abstract - The rheological behaviour of a commercial thermoplastic elastomer, CARIFLEX TR-1102, a block copolymer of the A-B-A type, has been studied by the IUPAC Working Party "Structure and Properties of Commercial Polymers". The behaviour was found to be quite different from that of otherwise similar random copolymers - the melt viscosity was much higher and measurements in the low shear rate range were poorly reproducible and highly sensitive to shear history. This behaviour can largely be explained in terms of structural changes taking place in the melt, the initial network structure being progressively disrupted by the shear stresses resulting at stresses above about 3000 Pa, in complete disruption of the network and the formation of a star-shaped branched structure. This latter structure is thought to be responsible for the build-up of a residual shear stress in stress relaxation experiments. All of these aspects are discussed in the following article.

C O N T E N T S

1. INTRODUCTION

At the end of 1973, the IUPAC Working Party on "Structure and Properties of Commercial Polymers" decided to start a programme on the rheology of thermoplastic elastomers to which class also belong the block copolymers of the A-B-A type. The rheological behaviour of such block copolymers is considerably different from that of homopolymers and random copolymers (Refs. 1-3). The block copolymers exhibit e.g. higher melt viscosities than random copolymers of the same molecular weight and the same composition and also do not exhibit a constant viscosity at low shear rates. This complex rheological behaviour is mainly attributed to the persistence of the two-phase domain structure of the block copolymers in the melt.

The objective of the present investigation is to study the effect of the domain structure on the rheological behaviour of one well defined commercially available thermoplastic elastomer, namely CARIFLEX TR-1102.

In all, 14 members of the Working Party participated in the programme. Table I shows a list of the participants in alphabetical order. The code given to the participants in Table I will be used in this report when reference is made to the results of a given laboratory. Table I also contains the symbols used in the figures presenting the results of a given laboratory.

TABLE 1. List of participants

Alphabetic code	Participant	Symbol in figures
A	BASF, Ludwigshafen, Germany	○
B	Borg Warner Chemicals, Amsterdam, The Netherlands	□
C	Firestone Tyre & Rubber Co., Akron, U.S.A.	◇
D	Hoechst AG, Frankfurt am Main, Germany	△
E	Chemische Werke Hüls AG, Marl, Germany	◁
F	ICI Plastics Division, Welwyn Garden City, England	▽
G	Industrial Chemistry Institute, Warsaw, Poland	▷
H	IKT, University of Stuttgart, Stuttgart, Germany	●
I	Institute of Petrochemical Synthesis, Moscow, USSR	■
J	Montedison S.p.A., Bollate and Ferrara, Italy	◆
K	Rheology Research Center, University of Wisconsin Madison, U.S.A.	▲
L	Rhône-Poulenc, Antony, France	◀
M	Shell, Amsterdam, The Netherlands	▼
N	TNO, Delft, The Netherlands	▶

2. DESCRIPTION AND PROPERTIES OF "CARIFLEX" TR-1102

CARIFLEX TR-1102 thermoplastic rubber is a commercial triblock copolymer of the styrene-butadiene-styrene (S-B-S) type manufactured by Shell. The nominal block lengths in molecular weight units are 11 000 - 56 000 - 11 000, i.e. the styrene percentage of the copolymer is about 28 %w. The molecular weight distribution of the block copolymer is relatively narrow ($\bar{M}w/\bar{M}n \simeq 1.2$).

The polystyrene and polybutadiene species are mutually incompatible, thus resulting in a two-phase structure. At room temperature, the hard and glassy polystyrene domains (polystyrene block T_g = +60 °C) are dispersed in a rubbery polybutadiene matrix (polybutadiene midblock T_g = -95 °C*). Owing to the molecular connection between the two species within a chain, the polystyrene domains act as crosslinks thus creating a network.

---

* DSC-measurements, Lab. M

According to theory (Refs. 4, 5), the two-phase morphology of SBS block copolymers depends upon the ratio of the butadiene block molecular weight to the styrene block molecular weight (M_B/M_S). The stable morphology of CARIFLEX TR-1102, for which M_B/M_S is around 5, is that of polystyrene cylinders in a polybutadiene matrix. Small angle X-ray and electron microscopy experiments by Keller et al (Ref. 6) have shown that in extruded CARIFLEX TR-1102 the polystyrene cylinders are hexagonally packed with the cylinder axis along the extrusion direction. The cylinders have a diameter of about 15 nm and a length of the order of $10^3 - 10^4$ nm. The scale of periodicity is about 30 nm.

Some other characteristic properties of CARIFLEX TR-1102 are density at 25 °C = 940 kg/m^3; melt index (G condition) = 9.7 g/10 min; gel content = < 0.01 %w.

3. THERMAL AND SHEAR STABILITY

3.1. Thermal stability

The polybutadiene midblock of the copolymer is, like polybutadiene homopolymer and other unsaturated polymers, very sensitive to oxidation. The oxidation reactions predominantly lead to cross linking rather than to chain scission of the molecules.

The TR rubber investigated in this programme contains 0.25 %w of IONOL (= 2,6-di-tert-butyl-4 methyl phenol) as an antioxidant to protect it against oxygen attack during manufacture, shipment and storage. This level and type of antioxidant, however, does not provide sufficient protection against oxidative attack at high temperatures: IONOL is a rather volatile substance with a melting point of 70 °C.

As the rheological properties will be influenced by the oxidation reactions, several laboratories have investigated the thermal stability of TR-1102 at different temperatures.

From results obtained by capillary and slit rheometry, it follows that at 150 °C a residence time of up to 2 h has no significant effect upon the measured viscosity (see, also, Figure 1). Also with other techniques (e.g. melt index apparatus) it was found that

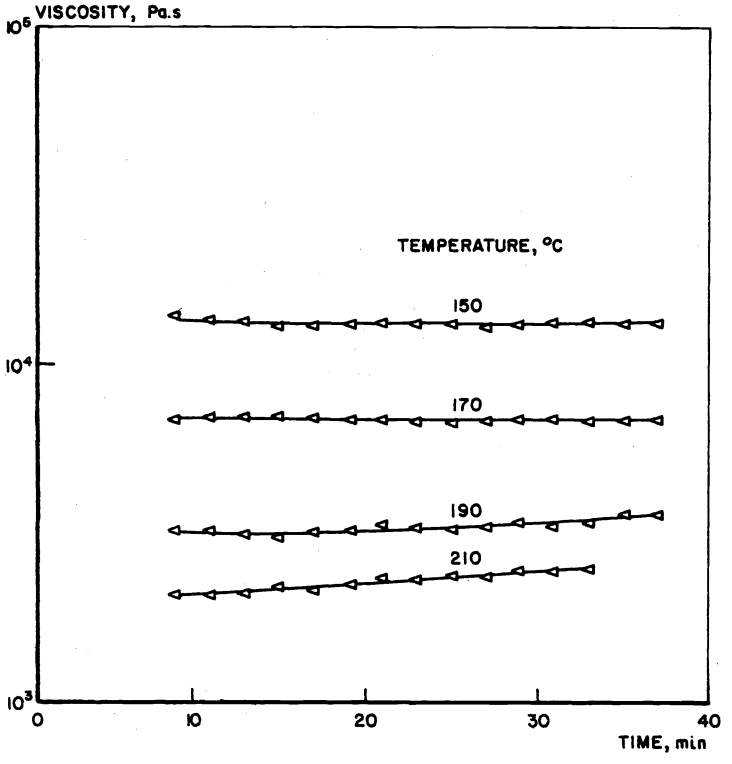

Fig. 1. Effect of residence time upon the viscosity at $\dot{\gamma}$ = 6.32 s^{-1} for different temperatures

a residence time of 2 h in the apparatus has no effect upon the measured values. With cone and plate viscometers, however, different results have been obtained as regards the thermal stability. Lab. A reported a thermal stability of at least 2 h in terms of the measured viscosity and Lab. E even reported a thermal stability of 8 h in terms of a solution viscosity and the gel content. Lab. M reported a much lower thermal stability at 150 °C. Using steady shear experiments, a continuous viscosity increase has been observed after a residence time of only 1 h. With oscillatory shear experiments, a 4 % increase in the storage modulus G' was found between measurements made 90 and 10 minutes after preheating the sample (preheating time = 30 min). This increase in G' was found to be dependent upon the amount of nitrogen flowing through the thermostat of the cone and plate viscometer (see Table 2).

TABLE 2. Effect of nitrogen flow rate and type of antioxidant upon thermal stability at 150 °C in cone and plate viscometer

Antioxidant	Nitrogen flow rate l/min	$G'_{t=90}/G'_{t=10}$	$G''_{t=90}/G''_{t=10}$	$\lvert\eta^*\rvert_{t=90}/\lvert\eta^*\rvert_{t=10}$
IONOL	8	1.04	1.03	1.04
IONOL	30	1.07	1.04	1.06
IONOX 330	30	0.99	1.07	1.02

The use of a higher melting antioxidant, IONOX 330 (melting point = 244 °C), on the other hand, hardly influences the storage modulus values. These results indicate that, in the cone and plate viscometer even at temperatures of 150 °C, the antioxidant IONOL evaporates during the measurements. In addition, brown coloured material was always present at the rim of the tested samples, which colour is probably caused by the oxidation products of IONOL. Both processes, evaporation and oxidation of IONOL at the rim of the cone and plate geometry, are considered to be responsible for the enhanced thermal instability in the case of cone and plate measurements compared to capillary experiments as observed by Lab. M. The fact that Lab. A and Lab. E have found a higher thermal stability than Lab. M, might be attributed to different experimental conditions (such as nitrogen flow rate and amount of oxygen in nitrogen).

At higher temperatures, the thermal stability of TR-1102 strongly decreases with increasing temperature. At 170 °C the thermal stability is still reported to be reasonable. Using capillary rheometry, no viscosity changes have been observed after residence times of 35 min (Lab. E, see also Figure 1) and 1 h (Lab. J). At 190 °C, again with capillary rheometry, Lab. E reported a viscosity increase of about 10 % after 35 min measurement (see Figure 1), whereas Lab. A reported no detectable viscosity change after 22 min. Using melt index and cone and plate measurements, Lab. A reported substantial changes in the measured values for a residence time of 2 h, i.e. for the melt index a change of a factor 3 and for the shear stress and the normal stress a factor of about 5. At 210 °C, finally, the thermal stability is very poor. Using capillary rheometry, Lab. E reported a viscosity increase of about 20 % after 35 min measurements, while Lab. D reported a significant increase in die swell values after 10 min measurements.

3.2. Shear stability

Using capillary experiments Lab. A has reported that a two-fold pre-extrusion at a shear rate of 20 s^{-1} at 150 °C does not change the flow behaviour of CARIFLEX TR-1102 in the shear rate range from 1 to 100 s^{-1}.

4. CAPILLARY MEASUREMENTS

Most participants in the programme have carried out viscosity and also extrudate swell measurements using capillary rheometry. Table 3 gives a survey of the type of instrument and the experimental conditions used. Most of the measurements by far were performed at a temperature of 150 °C.

TABLE 3. Equipment used for capillary rheometry experiments

Participant	Apparatus	Temperature °C	L/D ratio used	Corrected for Bagley
A	Nitrogen driven viscometer	150-190	6, 8, 12	yes
B	Instron capillary rheometer, Model 3211	110-210	40.6	no
		150	20-100	no
D	Modified melt indexer	110-190	20.5	Only at 150 °C
E	Zwick capillary rheometer	110-210	40	no
		150	20-40	no
F	Davenport capillary rheometer	150	16	yes pressure drop short die
G	MCR capillary rheometer	150	53	no
H	Slit die viscometer	150		yes
I	Constant pressure capillary	110-170	20.6	no
	rheometer	150	5-42	no
J	Göttfert capillary rheometer, Model HKV 2000	130	30, 40	no
		150	5-40	yes
		170	40	no
L	Instron capillary rheometer	130	5,10	yes
		150, 170	10-40	yes
		190	40	no
M	Instron capillary rheometer	110-190	40	no
		150	5-40	yes
N	Slit die viscometer	110-210		yes

4.1. Viscosity behaviour

4.1.1. Effect of shear rate (shear stress)

Fig. 2 shows the experimental viscosity-shear rate data at a temperature of 150 °C. For reasons of survey not all experimental data from one participant have been included. All data presented were corrected for non-parabolic flow profiles (Rabinowitsch correction). The data were also corrected for end effects (Bagley correction, see Table 3) or were obtained with capillaries having L/D ratios higher than 16 in which cases the Bagley correction is quite small. The effect of L/D ratio upon viscosity has been studied by various participants. Fig. 3 shows a Bagley plot obtained by Lab. J. It follows that the Bagley correction is generally quite small. Even at the highest shear rates used the correction (expressed in L/D values) is less than 1.

From Fig. 2 it follows that the agreement between the results of the various participants is quite satisfactory for the purpose of the present investigation. The scatter in the results is highest at the lower shear rates ($< 10\ s^{-1}$), in which region the results do not differ more than a factor 1.5.

As regards the shape of the flow curve at 150 °C, it follows that probably no constant viscosity exists at low shear rates (shear stresses). The slope $d \log \eta / d \log \dot{\gamma}$ is about -0.1 at shear rates lower than $10\ s^{-1}$. At high shear rates the viscosity strongly decreases with increasing shear rate; at shear rates higher than $100\ s^{-1}$ the slope $d \log \eta / d \log \dot{\gamma}$ is almost -1.

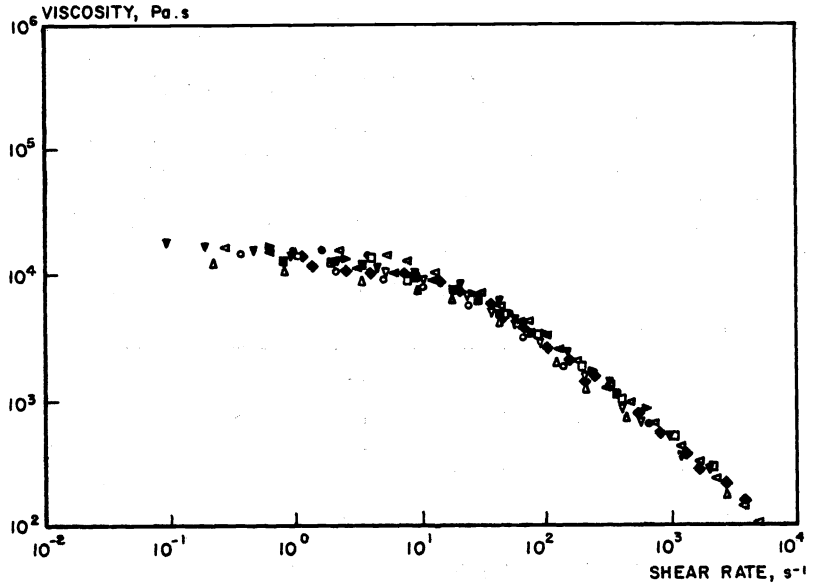

Fig. 2. Viscosity as a function of shear rate at 150 °C. Capillary rheometry data corrected for Bagley and Rabinowitsch

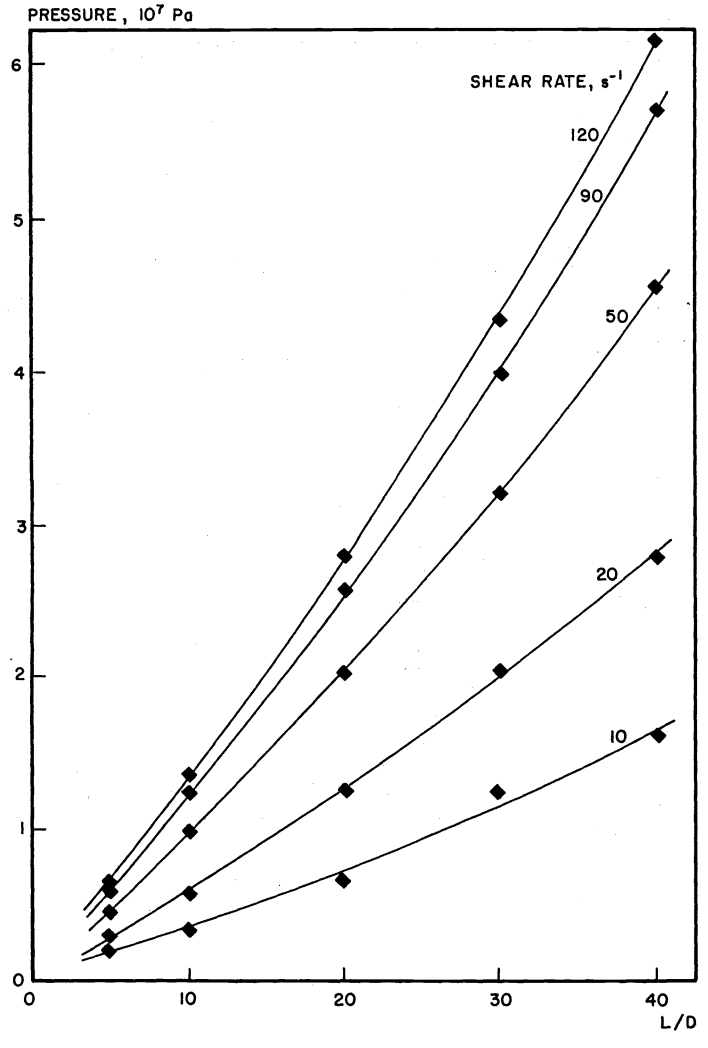

Fig. 3. Bagley plot at 150 °C for a range of shear rates

4.1.2. Effect of pressure

The effect of pressure upon viscosity was measured by Lab. F by means of a Couette-Hatschek viscometer (Ref. 7). Fig. 4 shows some typical results obtained at 1000 bar in comparison with results at atmospheric pressure at three temperature levels. From the results it follows that the flow curves at different pressures and temperatures can be superimposed by a shift at constant shear stress. The effect of pressure upon viscosity can therefore be expressed in terms of a temperature-pressure coefficient $\Delta T/\Delta P$. For CARIFLEX TR-1102 this coefficient is reported to be 6×10^{-7} °C/Pa, which means that pressurisation to 10^8 Pa (1000 bar) has the same effect upon viscosity as a temperature decrease of 60 °C.

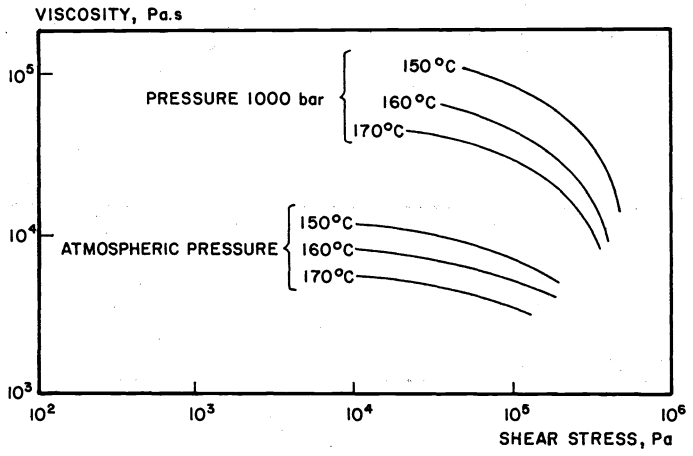

Fig. 4. Effect of hydrostatic pressure upon the viscosity at three temperature levels

The effect of pressure upon viscosity is also visible as a non-linearity in the Bagley plots as observed, for instance, by Labs. J and L (see also Fig. 3). Lab. J has used this non-linearity of the plots to calculate the pressure coefficient of the viscosity using the procedure described by Wales (Ref. 8). A pressure coefficient α of 4.15×10^{-8} Pa^{-1} has been found. This value is in reasonable agreement with an α value of 3×10^{-8} Pa^{-1} being derived from the $\Delta T/\Delta P$ value reported by Lab. F, using an activation energy of 18 kcal/mol. A similar difference in α values derived from the two methods has been reported by Wales for polyvinyl chloride (Ref. 8).

The viscosity data obtained by capillary rheometry have all been measured under rather high hydrostatic pressure, in contrast e.g. to viscosity data obtained by cone and plate measurements, which are always obtained under atmospheric pressure. As the various participants, moreover, have used capillaries with different L/D ratios for their measurements, the viscosity values presented in Fig. 2 were thus measured under different hydrostatic pressure. Part of the scatter in the viscosity data of Fig. 2 can be attributed to these hydrostatic pressure differences. For these reasons, the viscosity data of Fig. 2 were normalised to atmospheric pressure using an α value of 3×10^{-8} Pa^{-1}. The normalised viscosity data are given in Fig. 5. All experimental data are included in this figure. From Fig. 5 it follows that the scatter in the normalised viscosity data is, indeed, slightly smaller than the scatter in the non-normalised data.

4.1.3. Effect of temperature

Figs. 6 A/E show the viscosity-shear rate obtained at 110, 130, 170, 190 and 210 °C, respectively. The Rabinowitsch correction was used with all data. In addition, all data either were subjected to the Bagley correction or were obtained with capillaries having L/D ratios higher than 20.

From Figs. 6 A/E it follows that at all the temperatures studied the scatter in the viscosity data of the various participants is again higher at the lowest rates of shear. Furthermore, the scatter is higher at the lower temperatures 110 and 130 °C and also at the highest temperature of 210 °C; at 210 °C, the thermal stability of the material is very poor.

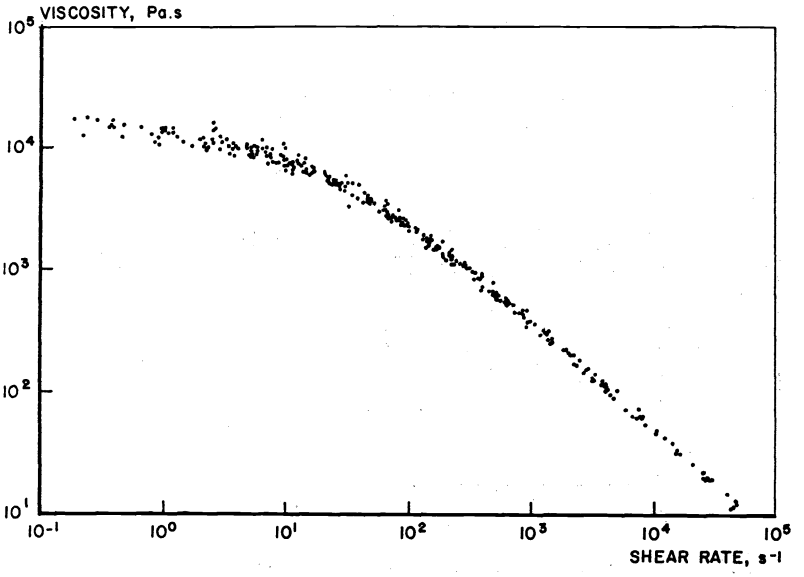

Fig. 5. Viscosity as a function of shear rate at 150 °C. Capillary rheometry data normalised to a pressure of 1 bar

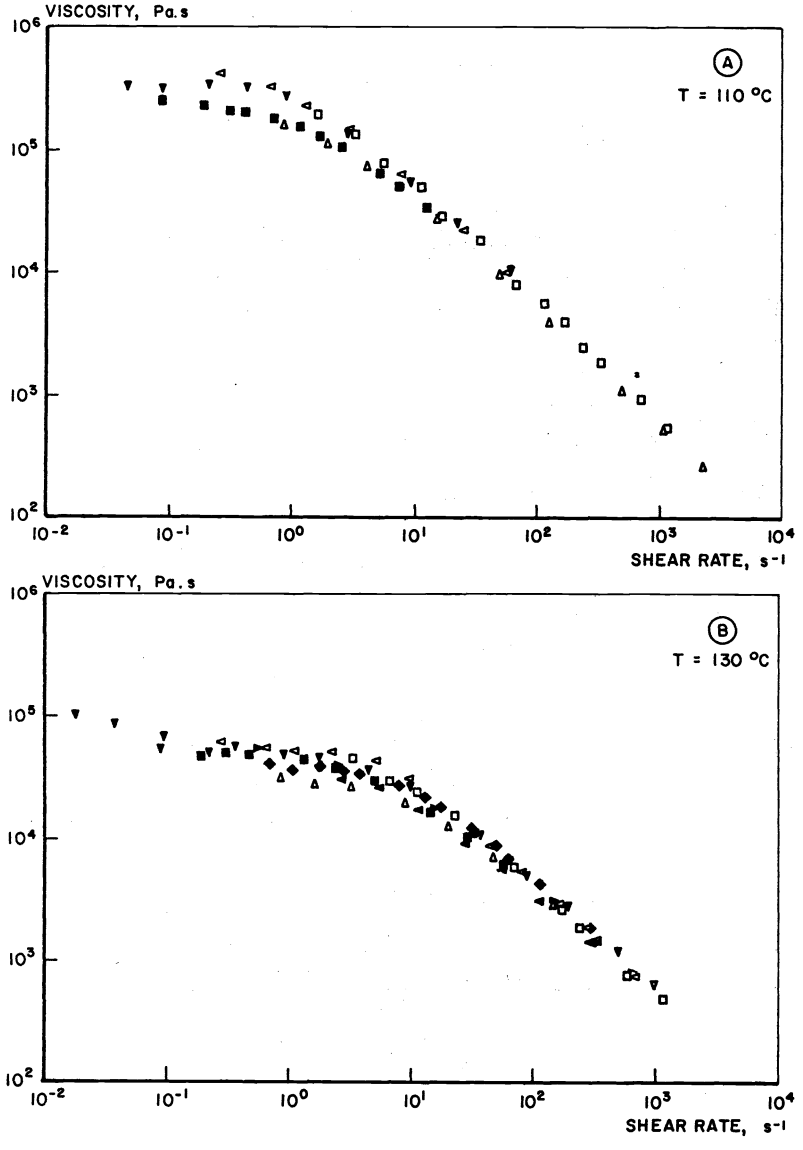

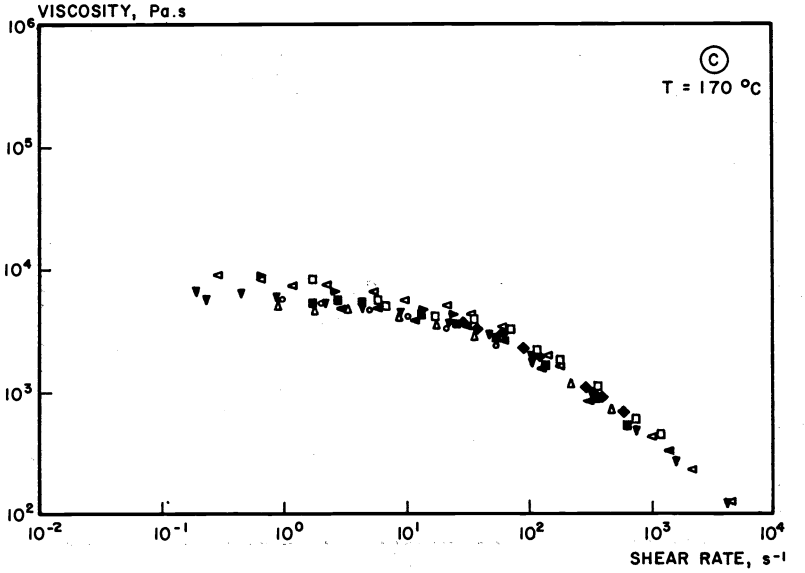

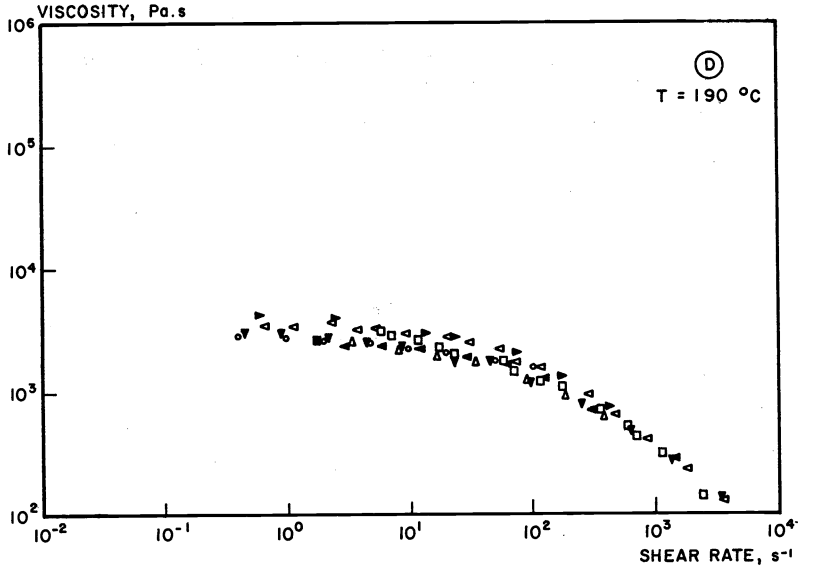

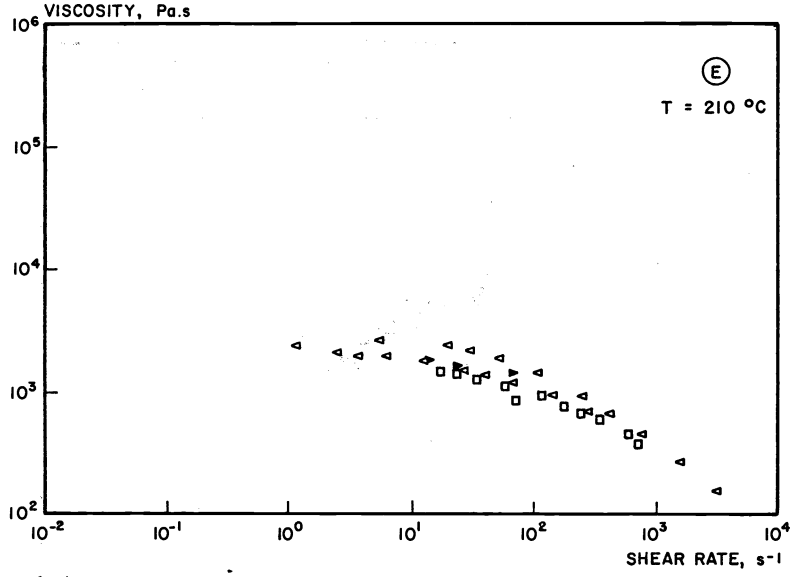

Figs. 6A/E. Viscosity as a function of shear rate at different temperatures. Capillary rheometry data

Fig. 7 shows the temperature dependence of the viscosity at a shear stress level of 10^4 Pa, at which level the viscosities are almost independent of shear stress. For the construction of this Arrhenius plot the data of only one participant (Lab. M) were used, because of the scatter in data obtained by the various participants. As the flow curves at the various temperatures can be shifted (at constant shear stress) to a single mastercurve, the same temperature dependence is valid over the entire shear stress range. Fig. 7 also shows as a comparison the temperature dependence of the zero shear melt viscosities of polybutadiene (Ref. 9), polystyrene (Ref. 10) and of a butadiene/styrene (75/25) random copolymer (Ref. 11), all of the same molecular weight.

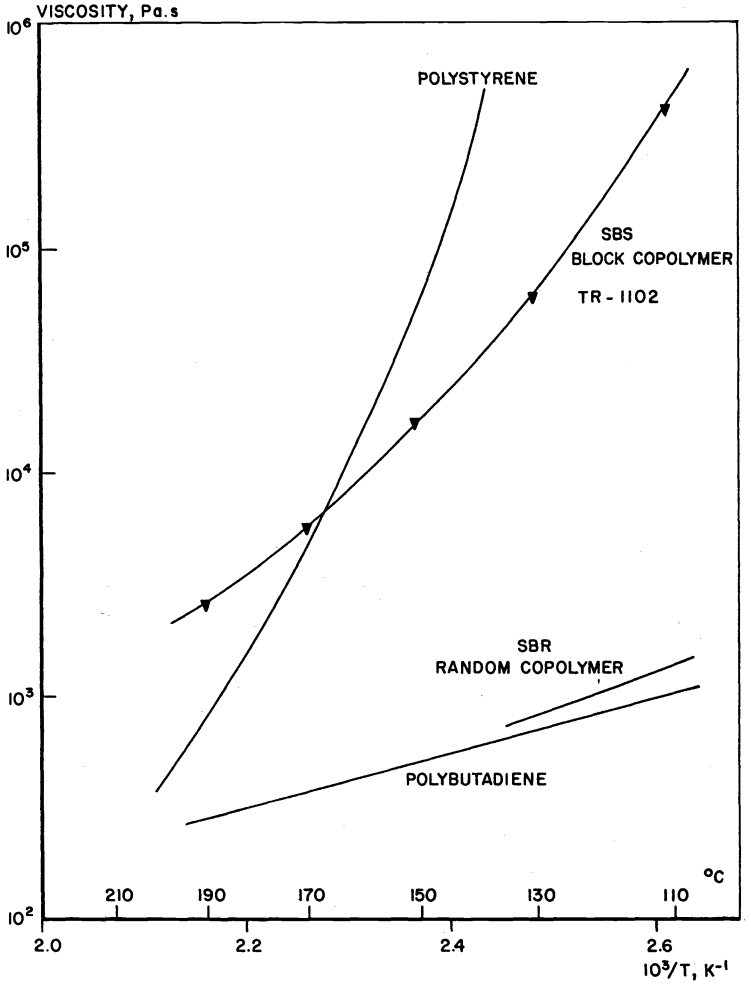

Fig. 7. Temperature dependence of the viscosity of the SBS block copolymer in comparison with that of a polybutadiene, a polystyrene and an SBR random copolymer of the same molecular weight. Viscosities of TR-1102 are taken at a shear stress of 10^4 Pa. The other viscosities are all zero-shear viscosities

It follows from Fig. 7 that the viscosity of the SBS block copolymer does not follow an Arrhenius type of temperature dependence over wide intervals in T.
The activation energy E, being calculated from the equation

$$E = R \, d \ln \eta / d (1/T)$$

in fact, increases with decreasing temperature. At temperatures between 170 and 190 °C, E is about 15 kcal/mole whereas, at temperatures between 110 and 130 °C, E is about 30 kcal/mole. This high activation energy at low temperatures is at least partly responsible for the observed large scatter in the viscosity data at 110 °C and 130 °C.

It follows furthermore from Figure 7 that the viscosities of the polybutadiene and of the SBR random copolymer are very low and only slightly dependent on temperature, which is related to the fact that both polymers have a very low T_g value. Both polystyrene and the SBS block copolymer have a much higher viscosity and are much more sensitive to temperature, which is related to the relatively high T_g values of polystyrene and of the polystyrene endblock of the copolymer. As a consequence of the somewhat lower T_g value of the polystyrene endblock of the copolymer (T_g = ca. 60 °C) compared to that of polystyrene (T_g = ca. 110 °C), the viscosity of the block copolymer is lower than that of polystyrene at low temperatures. At higher temperatures these differences are outweighed by the viscosity increasing effect of the polystyrene domains (still present at 10^4 Pa) upon the viscosity of the block copolymer. It should be noted, however, that in order to assess the effect of domain structure upon the viscosity level of TR-1102, it would be necessary to compare the viscosities of TR-1102 with those of the other polymers at corresponding states, e.g. at equal values of T/Tg.

4.2. Extrudate swell behaviour

Most participants who have measured the viscosity behaviour have also measured the diameter of the extrudates after cooling to room temperature. A few have annealed their extrudates at 150 °C in silicone oil or polyethylene glycol before measurement but no significant effect of annealing was found. In the case of "sharkskin", which is present on the extrudates at shear stresses higher than about 10^5 Pa, the extrudate diameter measured was the maximum one. No corrections were made for the volume contraction occurring in cooling the extrudates to room temperature. This correction would result in ca. 3 % higher values of the diameter of the extrudates.

4.2.1. Effect of shear stress

Fig. 8 shows a plot of the extrudate swell ratio d/d_o (d = extrudate diameter, d_o = die diameter) versus shear stress for a temperature of 150 °C and an L/D ratio of 10. The shear stress values were corrected for entrance pressure losses (Bagley correction). As a comparison Fig. 8 also shows the extrudate swell results (corrected for volume contraction) of a very narrow molecular weight distribution polystyrene of comparable total molecular weight, being derived from data of Graessley et al (Ref. 12). It follows from Fig. 8 that the swell ratio is very low (about 1.04) at low shear stresses ($< 10^5$ Pa, $\dot{\gamma} < 10\ s^{-1}$), but strongly increases with increasing shear stress above 10^5 Pa.

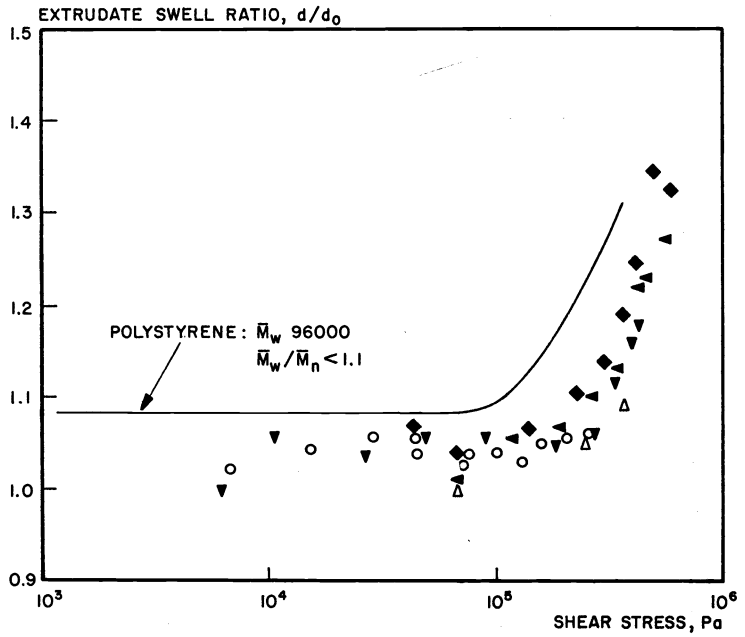

Fig. 8. Extrudate swell ratio as a function of shear stress at 150 °C for an L/D ratio of 10. Extrudate swell data of a polystyrene are also given

4.2.2. Effect of L/D ratio

The effect of L/D ratio upon extrudate swell compared at constant shear stress is found to be small at high L/D ratios (20 to 40). Below an L/D ratio of about 20, the swell ratio slightly increases with decreasing L/D.

4.2.3. Effect of temperature

In the range of 110 to 210 °C the extrudate swell has been found to be nearly independent of temperature, provided swell ratios are compared at constant shear stress.

5. STEADY SHEAR EXPERIMENTS IN CONE AND PLATE FLOW

Various participants have performed cone and plate experiments for determining the steady-state viscosity at relatively low shear rates. In addition, the shear stress relaxation behaviour and normal stresses were also measured in some cases. Most of the measurements were carried out at a temperature of 150 °C. Table 4 gives a survey of the instruments and experimental conditions used.

TABLE 4. Equipment used for steady-shear experiments

Participant	Apparatus	Cone and plate dimensions	
		Platen diameter, mm	Cone angle, degree
A	Weissenberg rheogoniometer	24	8
E	Weissenberg rheogoniometer	25	2.02
F			5
J	Weissenberg rheogoniometer	50	2.01
L	Rheometrics mechanical spectrometer	25	2.29
M	Weissenberg rheogoniometer	25	3.97

5.1. Shear stress build up

5.1.1. Effect of shear rate

Fig. 9 shows some typical shear stress-time traces obtained by Lab. A and Lab. M at different rates of shear. Other participants also have reported the same type of traces (Lab. F and Lab. L) although e.g. the height of the maximum in the traces can differ considerably. From Fig. 9 it follows that depending on the shear rate the traces have a very different shape. At low shear rates ($\dot{\gamma} \approx 0.001\ s^{-1}$) the shear stress reaches a more or less steady value after 10 min but thereafter again increases with time. At intermediate shear rates (from 0.001 up to 1 s^{-1}), the shear stress first passes through a more or less pronounced maximum and then continuously decreases with time. Lab. M reported this decrease in shear stress to be followed by an increase in shear stress probably due to the thermal instability of the sample (see also section 3.1). At the higher shear rates ($\dot{\gamma} = 1.8\ s^{-1}$) the maximum is no longer present and the torque decreases right from the start of the experiment. This decrease in torque is ascribed to shearing out of the sample, which effect has also been visually observed at still lower shear rates (down to $\dot{\gamma} = 0.01\ s^{-1}$). Similar observations were made by Chung and Gale (Ref. 13) who have reported that even at shear rates of $8.5 \times 10^{-4}\ s^{-1}$ SBS samples show a tendency to cavitate and climb out of the cone and plate gap. From the traces presented in Fig. 9, it is evident that over the whole shear rate range no steady value is reached for the shear stress. The calculation of viscosity consequently becomes rather arbitrary. The various participants, in fact, have used shear stress values from different positions on the traces to calculate viscosity. Lab. J, for instance, has used the shear stress values at the maximum, Lab. K has taken the shear stress after specified times (between 1 and 4 min) depending upon the shear rate, whereas Lab. A, E and M have taken the shear stress in the region where the changes in shear stress were small (times between 20 and 40 min). At very high shear rates ($\dot{\gamma} > 1.8\ s^{-1}$) Lab. M has taken the maximum of the curve as the shear stress.

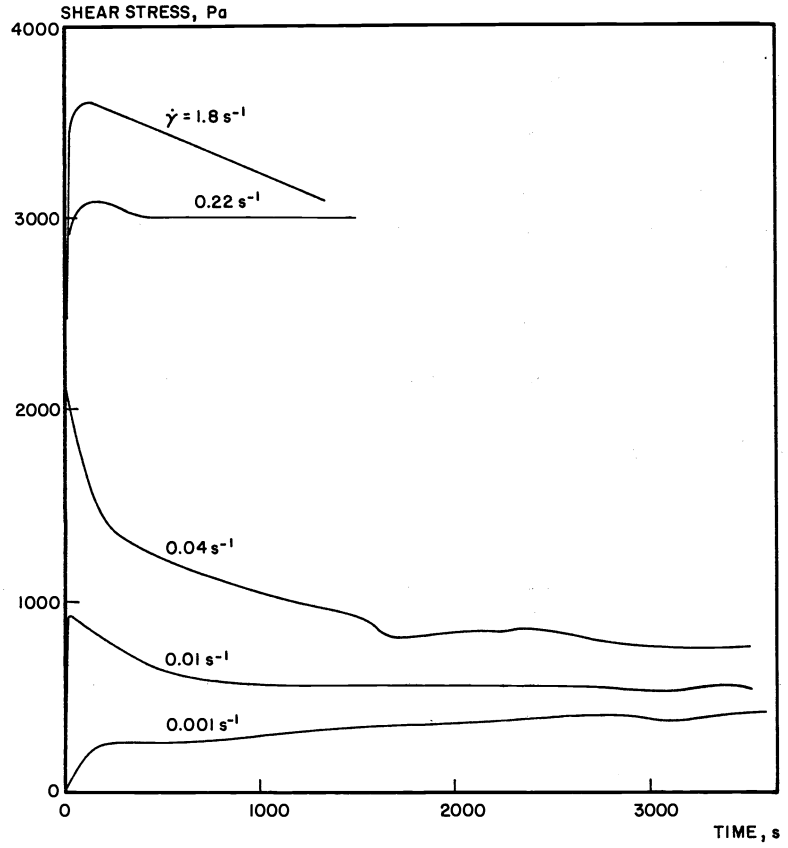

Fig. 9. Typical shear stress-time traces at 150 °C. Data of Lab. A and Lab. M

Figure 10 shows the calculated viscosities as a function of shear rate. The scatter in the results between the various participants is indeed quite considerable and can partly be explained by the different evaluation of the traces. A large part of the observed spread in the results should also be attributed to the different sample preparation and the different experimental conditions (such as gap setting procedure, preheating time,

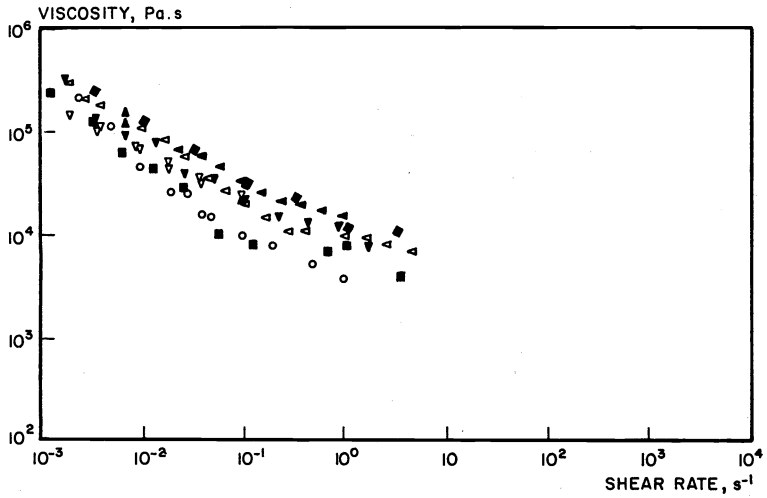

Fig. 10. Viscosity as a function of shear rate at 150 °C. Cone and plate measurements

shear history etc.). The effect of different experimental conditions, for instance, is demonstrated by the results of Lab. E in Figure 11. The upper curve was obtained with

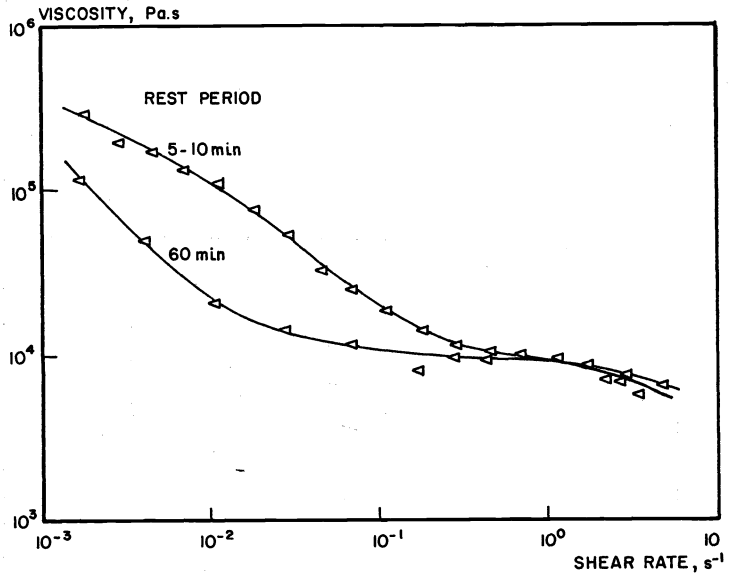

Fig. 11. Viscosity as a function of shear rate at 150 °C. Curves are obtained with different rest periods between successive cone and plate measurements

rest periods of 5-10 min between successive measurements, whereas the lower curve was obtained with a much larger rest period (60 min). It is of interest to note that the differences in the viscosity are greatest at the lower shear rates ($\dot{\gamma} < 0.1$ s^{-1}). As regards the effect of sample preparation, it has been found by Lab. M that the use of crumbs leads to less reproducible results for the viscosity at 0.01 and 0.1 s^{-1} than the use of compression moulded samples (see Table 5). The sensitivity of the viscosity

TABLE 5. Effect of sample preparation upon the viscosity values at two different shear rates. Cone and plate measurements at 150 °C

Sample preparation	Shear rate, s^{-1}	Number of observations	Viscosity, Pa.s	
			Mean value	Standard deviation
Crumbs	0.113	10	1.37×10^4	1.19×10^3
Compr. moulded	0.113	5	1.29×10^4	4.97×10^2
Crumbs	0.0113	10	7.41×10^4	8.63×10^3
Compr. moulded	0.0113	5	7.26×10^4	6.15×10^3

behaviour for the whole sequence of sample treatments (preparation and testing) still more clearly follows from the results for the shear stress-time dependence presented in Fig. 12. These results were obtained on compression moulded samples prepared and measured under nearly identical conditions. It follows that there is still a considerable spread between the results of the various participants, especially at the lowest shear rate of 0.01 s^{-1}. This also holds for the results obtained by only one participant (Lab. L, see also Fig. 12 and Lab. M, see Table 5). The fact that the observed spread in the results decreases as the shear rate increases explains also the findings of Lab. K that replicate measurements for the shear stress at $\dot{\gamma} = 1$ s^{-1} generally do not vary more than 5 % from the mean value. As regards the shape of the flow curve as determined by cone and plate measurements in steady shear flow, it follows from Fig. 10 that the viscosity at shear rates lower than 0.1 s^{-1} strongly increases with decreasing shear rate; the bilogarithmic slope d log η/d log $\dot{\gamma}$ in this region is about -0.6.

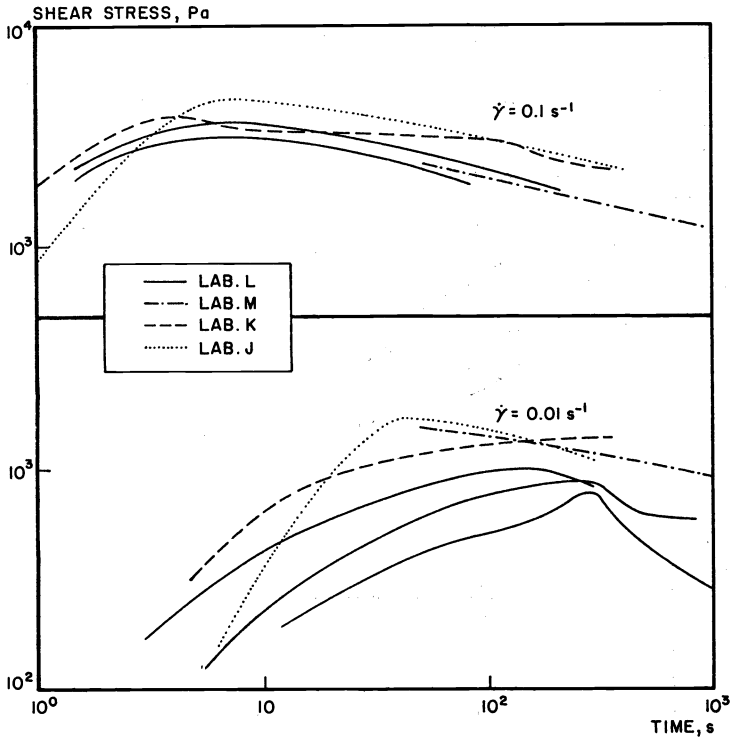

Fig. 12. Shear stress-time traces at 150 °C for two different shear rates

At shear rates higher than about 0.3 s^{-1} the viscosity shows the trend to become much less dependent upon the shear rate. This is, however, much more clearly shown by the capillary rheometry data from Fig. 2, which indeed agree well with the cone and plate results.

5.1.2. Effect of temperature

Fig. 13 shows the viscosity-shear rate data obtained at 130 °C and 170 °C. It follows that the shape of the curves is similar to that observed at 150 °C, i.e. also at these temperatures two regions of response can be distinguished. The constant slope of the curve at low shear rates (shear stresses < ca. 3 x 10^3 Pa) appears to be independent of temperature in the region of 130 to 170 °C.

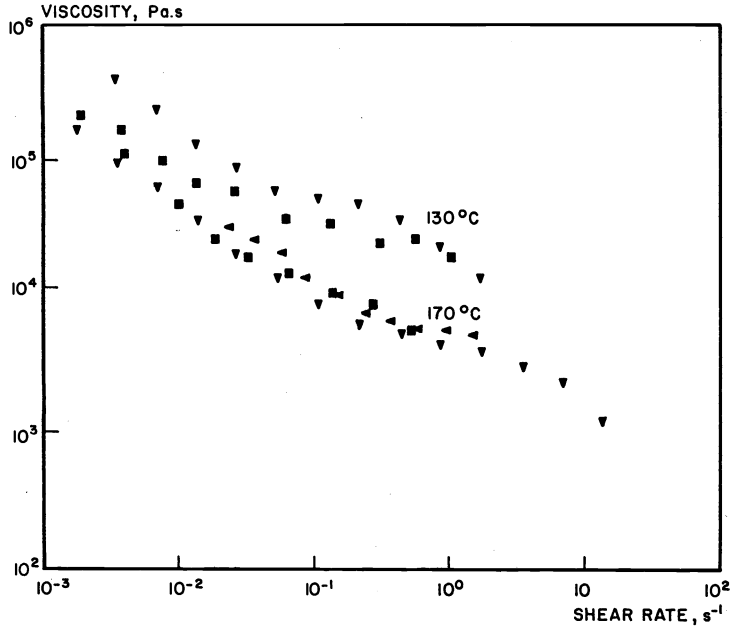

Fig. 13. Viscosity as a function of shear rate at 130 and 170 °C. Cone and plate measurements

5.2. Shear stress relaxation

Fig. 14 shows a typical result of a relaxation curve obtained by Lab. A after the cessation of steady shear (shear rate = 0.01 s^{-1}, time of shear = 1 h). It follows from this Figure that the shear stress does not achieve complete relaxation, but approaches a nearly constant value P_{12}^{∞}. Similarly it was observed by Lab. N that also the flow birefringence does not relax completely. This residual shear stress was found to be independent of shear rate in the range from 10^{-3} up to 1 s^{-1} at a constant deformation time of one hour. Lower values

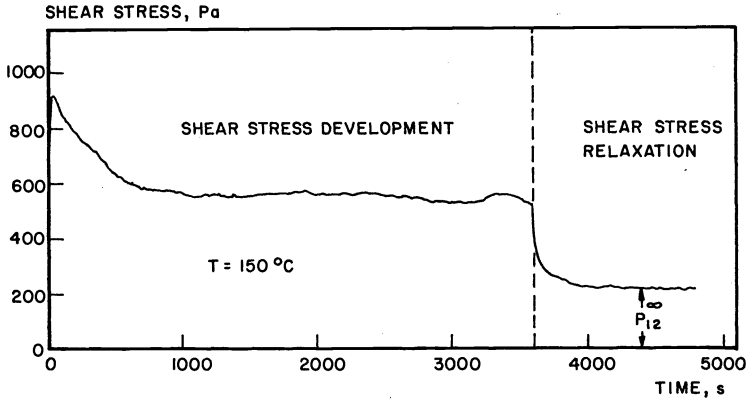

Fig. 14. Shear stress development at a shear rate of 0.01 s^{-1} followed by shear stress relaxation. Data of Lab. A

for P_{12}^{∞}, however, were found when the time of previous shear deformation was reduced from 1 h to 1000 s. This latter result is also confirmed by data of Lab. K obtained at a shear rate of 0.1 s^{-1} and times of shear of 50 and 350 s (see Fig. 15). Lab. J, which has carried out relaxation experiments by stopping the rotation of the cone when the shear stress reaches its maximum value (after 1-30 s), has observed still much lower values for the residual shear stress (see, for instance, Fig. 16 and compare with Fig. 14). The results of Labs. A, K and J thus indicate that the residual shear stress strongly depends on the time of previous shear deformation. In addition, both Lab. K and Lab. J have found that the rate of shear stress relaxation increases as the rate of previous shear increases.

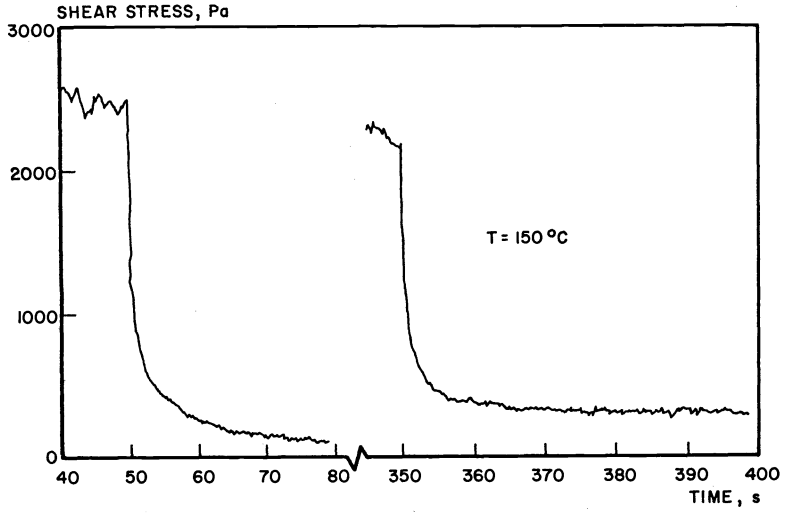

Fig. 15. Shear stress relaxation curves after different times of previous deformation at a shear rate of 0.1 s^{-1}. Data of Lab. K

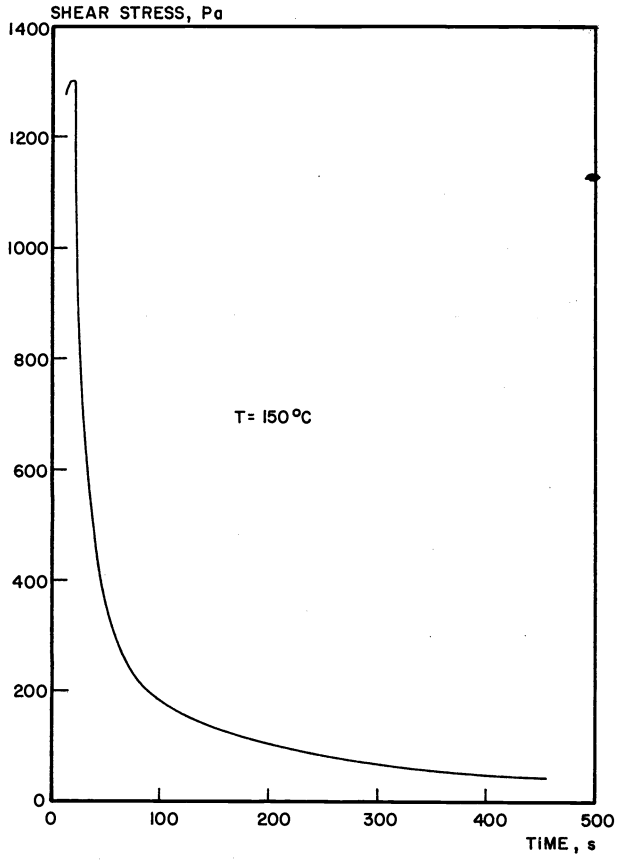

Fig. 16. Shear stress relaxation after reaching the maximum shear stress at a shear rate of 0.0112 s^{-1}. Data of Lab. J

5.3. Normal stresses

The time dependence of the first normal stress difference $P_{11} - P_{22}$ was measured by a few participants. Fig. 17 shows some results obtained at a shear rate of nominally 1 s^{-1}. The

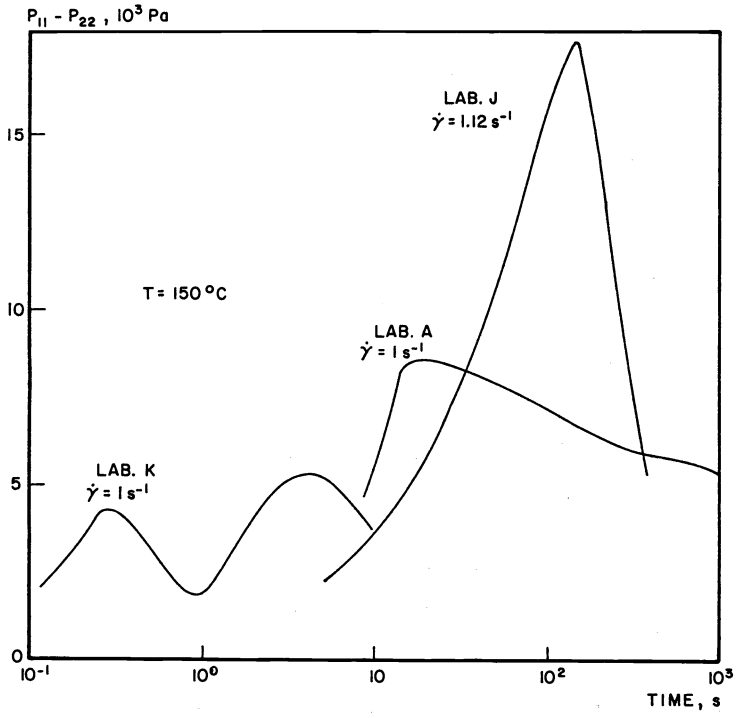

Fig. 17. Typical traces of the first normal stress difference versus time at a shear rate of nominally, 1 s^{-1}

different shape of the traces is quite obvious. Lab. K observed a double maximum, which could qualitatively be reproduced in replicate tests and which was also present at lower shear rates. Lab. J, on the other hand, always observed a very pronounced maximum followed by a rapid decrease of the normal stress. At shear rates lower than 1 s^{-1} Lab. J found that the normal stress even goes to zero after passing the maximum. A similar behaviour was observed by Lab. L as shown in Fig. 18. Lab. K even found that the thrust sometimes becomes negative during shearing at low shear rates. At shear rates higher than 1 s^{-1} both Lab. A and Lab. E have found less pronounced maxima followed by a more or less steady value of the normal stress. Just as in the case of shear stresses also in the case of normal stresses the scatter in the results is found to be much higher at low shear rates.

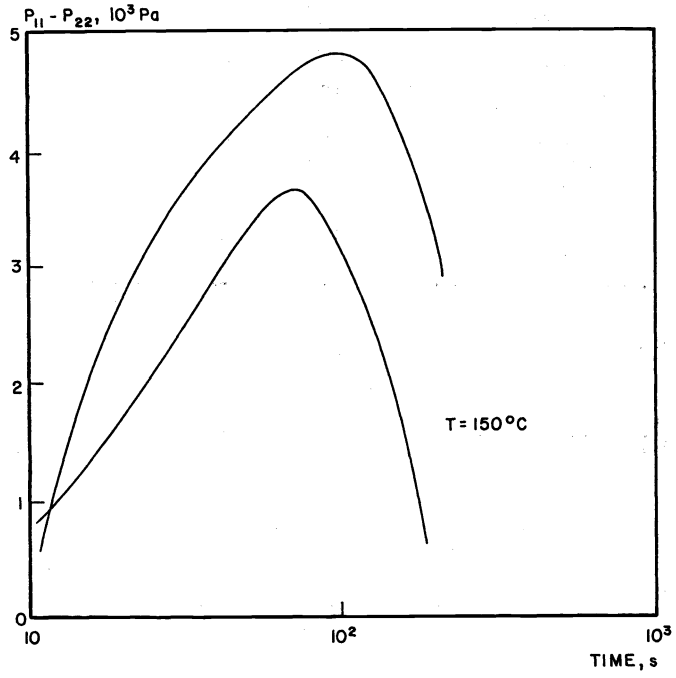

Fig. 18. Traces of the first normal stress difference versus time at a shear rate of 0.1 s^{-1}. Data of Lab. L

6. OSCILLATORY SHEAR EXPERIMENTS

A number of participants have carried out oscillatory shear experiments on compression moulded samples at a temperature of 150 °C. Table 6 gives a survey of the instruments and experimental conditions used. Fig. 19 shows the results, plotted as the complex viscosity $|\eta^*| = \{(\eta')^2 + (\eta'')^2\}^{\frac{1}{2}}$ as a function of angular frequency ω. In cases where replicate measurements were carried out, the average values are presented. Replicate measurements do not differ more than 20 % for most participants. The complex viscosity $|\eta^*|$ rather than the dynamic viscosity $\eta'(G''/\omega)$ is plotted in Fig. 19, as it has been found for several homopolymers and random copolymers that the complex viscosity as a function of ω coincides very well with the steady-shear viscosity as a function of $\dot{\gamma}$ when compared at $\omega = \dot{\gamma}$ (relation of Cox and Merz, Ref. 14). From Figure 19 it follows that the agreement between the results of the various participants is satisfactory. Only the results of Lab. C somewhat differ from those of the others. These deviating results of Lab. C cannot be ascribed to the differences in strain amplitude (compare Table 6), as it has been found by various laboratories (Labs C, L and M) that the effect of strain amplitude in the range 0.01 up to 0.2 is negligible. Considerable deviations from linear behaviour were only observed at strain amplitudes greater than 0.2 (results of Lab. C and Lab. I).

TABLE 6. Equipment used for oscillatory shear experiments

Participant	Apparatus	Type of geometry	Dimensions		Strain amplitude
			Platen diameter, mm	Cone angle, degree	
C	Rheometrics mechanical spectrometer	Eccentric disks			0.01-1.0
D	Weissenberg rheogoniometer	Cone and plate	50	2.0	0.1
I	Mechanical spectrometer	Concentric cylinders	*		< 0.02
L	Rheometrics mechanical spectrometer	Eccentric disks	25		0.1, 0.2
M	Weissenberg rheogoniometer	Cone and plate	25	1.99	0.023,0.23

* diameter outer cylinder = 12 mm, diameter inner cylinder = 6 mm and height = 20 mm

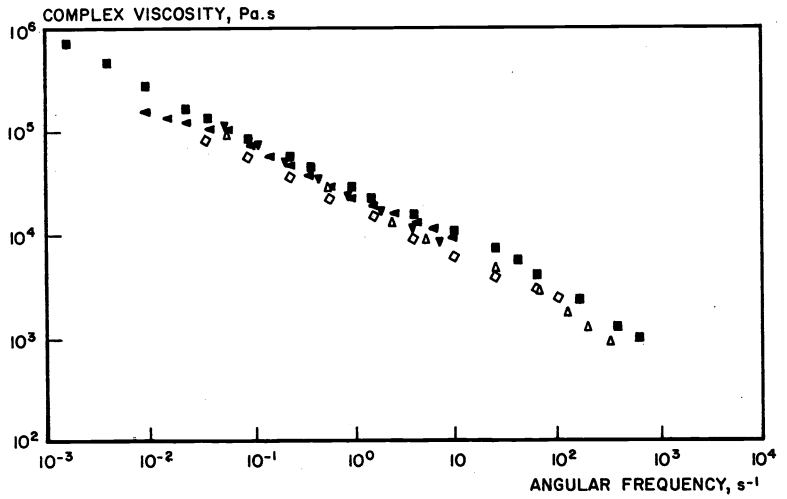

Fig. 19. Complex viscosity as a function of angular frequency at 150 °C

Comparing the results for the complex viscosity with the viscosity results obtained in steady shear at identical values of $\dot{\gamma}$ and ω it follows that at low shear rates (frequencies), $\dot{\gamma} < 1\ s^{-1}$, the complex viscosity is considerably higher (up to a factor 7) than the steady-shear viscosity. Similar results were obtained by Kraus et al (Ref. 15) for several linear and star-shaped branched block copolymers of styrene and butadiene. The slope $d \log|\eta^*| / d \log \omega$ at low frequencies is about -0.5 and is thus almost equal to the corresponding slope of the steady-shear viscosity data. Kraus and Gruver (Ref. 1) have observed similar values for the slope $d \log|\eta^*| / d \log \omega$ and have also reported that this slope depends upon the molecular weight of the polystyrene segments.

In addition to the complex viscosity data, Figure 20 shows a complete set of oscillatory shear results, i.e. the dynamic viscosity η' and the loss factor $\tan \delta$ (= G"/G') as a function of angular frequency ω. There is an obvious maximum in the $\tan \delta$ curve at about $\omega = 10\ s^{-1}$ which corresponds with an inflection point in the η' curve. Similar results were obtained by Arnold and Meier (Ref. 3), who have attributed this to the presence of a structural transition in the material.

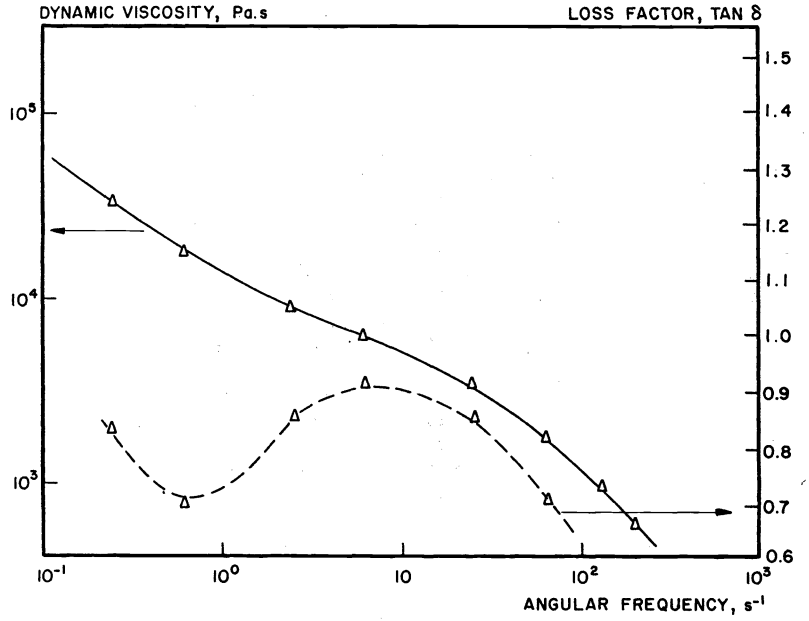

Fig. 20. Dynamic viscosity and loss factor as a function of angular frequency at 150 °C

7. SPECIAL EXPERIMENTS INVOLVING STEADY AND OSCILLATORY SHEAR

A few participants have carried out a number of special experiments in order to get information about the effect of shear history upon viscosity behaviour.

Fig. 21 shows some results of Lab. L and Lab. I obtained by cone and plate experiments in steady shear. The results given in Fig. 21A show that the viscosities measured with increasing shear rate from 2.5 x 10^{-2} up to 1 s^{-1} considerably differ from those measured with decreasing shear rate. Differences are greatest at low shear rates; at a shear rate of 2.5 x 10^{-2}, the values differ by about a factor of 2. Similar results as presented in Fig. 21A were obtained by Lab. F, where, however, a viscosity decrease was found at low shear rates of even a factor 5. Lab. F also found that this reduced viscosity increased with time and reached the original value of the fresh sample after resting for about four hours. This large effect of shear history upon the measured viscosities is even more clearly illustrated by the results of Lab. I as presented in Fig. 21B.

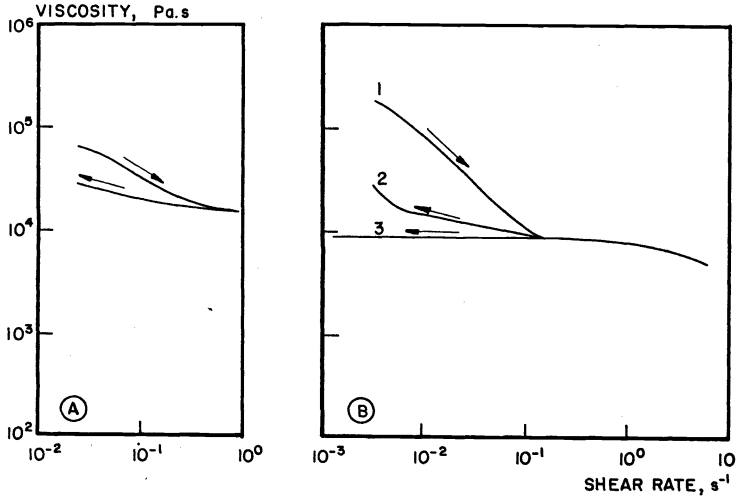

Fig. 21. Effect of shear history upon viscosity data at 150 °C. Cone and plate measurements of Lab. L (Fig. 21 A) and Lab. I (Fig. 21 B)

Fig. 21B shows the results of three different experiments, one with increasing rate of shear starting at 3.4×10^{-3} s^{-1} (experiment 1) and the others with decreasing rates of shear starting at different high shear rates ($\dot{\gamma} = 6.8 \times 10^{-1}$ s^{-1} for experiment 2, and $\dot{\gamma} = 1.1$ s^{-1} for experiment 3). It follows that, depending upon the shear history, the viscosity at a shear rate of 3.4×10^{-3} s^{-1} is as much as 25 times under that of a fresh sample. Possible causes for the observed reductions in viscosity are structural breakdown of the sample and shearing of the sample out of the gap. It will be clear, however, that viscosity reductions of the order of a factor 25 can only for a small part be attributed to shearing out of the sample. Structural breakdown of the sample, therefore, seems to play the most important role. Like Lab. F, Lab. I also observed that the viscosity decrease, measured at low shear rates, due to previous shearing at high shear rates is followed by considerable viscosity increases during rest (a factor 10 in 2 hours). Also from these results it is again evident that it is very difficult to obtain reproducible viscosity data in the low shear region, $\dot{\gamma} <$ ca. 1 s^{-1} (cf. reproducibility data of section 5.1).

In addition to the experiments of the Labs. F, I and L, Lab. M has studied the effect of shear history upon the viscosity behaviour at much lower levels of shear rate ($\dot{\gamma}$ from 10^{-3} to 10^{-1} s^{-1}) and shear strain (γ from 0 to 3). These experiments were performed in the following sequence: preheat for 30 min; small amplitude oscillatory shear for 10 min; apply well-defined magnitude of shear; small amplitude oscillatory shear, up to a total test time of 90 min. Small amplitude oscillations (a = 0.1, $\omega = 0.1$ s^{-1}) were used for determining the viscosity changes so as to prevent shearing out of the sample and also because it was expected that small amplitude oscillations would hardly lead to structural breakdown of the sample. The results obtained by Lab. M are summarised in Fig. 22, in which the viscosity changes are given as the ratio of the complex viscosities after 90 and 10 minutes testing. It follows from this figure that small amounts of shear strain ($\gamma \leqslant 0.5$), independent of the shear rate, already reduce the viscosity. Even the detection method itself was observed to have some effect. In reality, the effects are still somewhat greater than observed, as a residence time of 80 min at 150 °C itself leads to a 4 % increase in viscosity (cf. Table 2). Much more dramatic viscosity decreases (up to a factor 4) have been observed when using a high amplitude oscillation (a = 1, $\omega = 0.1$ s^{-1}) for 10 min.

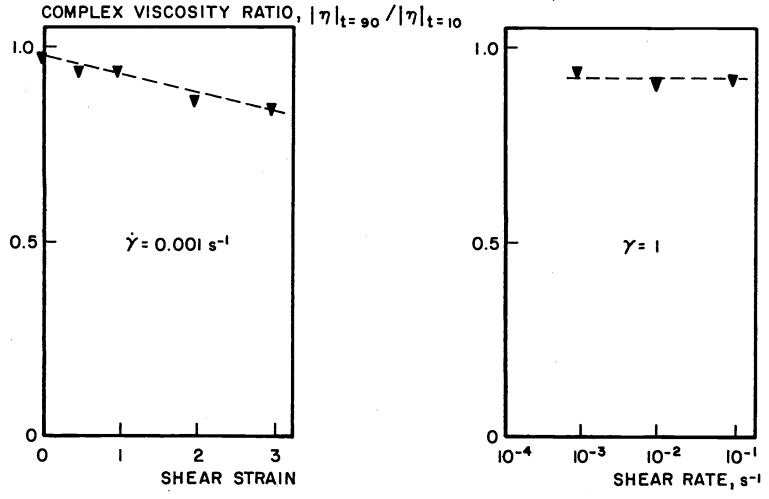

Fig. 22. Effect of shear history upon complex viscosity data at 150 °C at low levels of shear strain

Using a comparable detection method, Lab. D has found that the application of a high frequency, small amplitude, oscillation (a = 0.1, $\omega = 314$ s^{-1}) for 1 min lowers the complex viscosity by about 8 %.

8. CREEP MEASUREMENS IN SHEAR

Lab. A and Lab. I carried out creep measurements at constant shear stress on compression moulded samples at a temperature of 150 °C. The viscosities calculated from the creep data are presented in Fig. 23. For comparison, the average viscosity values obtained by cone and plate measurements in steady shear flow are also given in Fig. 23 (dashed line). There is a good agreement between the results obtained from the two methods.

The slope d log η/d log $\dot{\gamma}$ of the creep data is also -0.6, which means that the already observed viscosity behaviour at low shear rates appears to persist down to a shear rate of 10^{-5} s^{-1}.

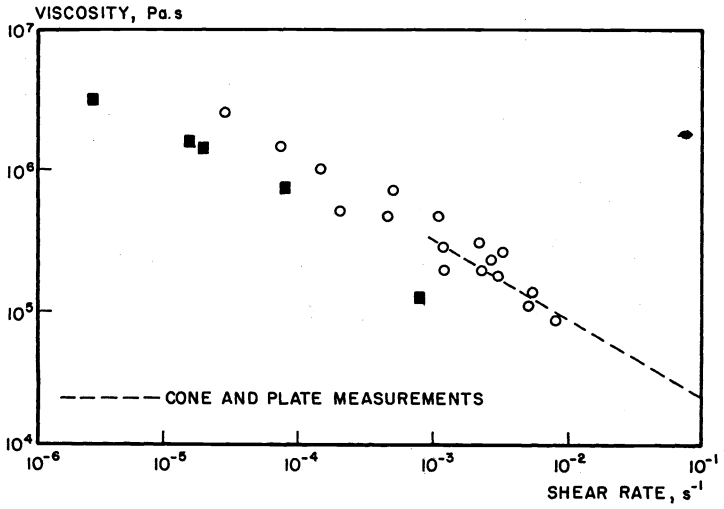

Fig. 23. Viscosity as a function of shear rate at 150 °C. Creep measurements in shear

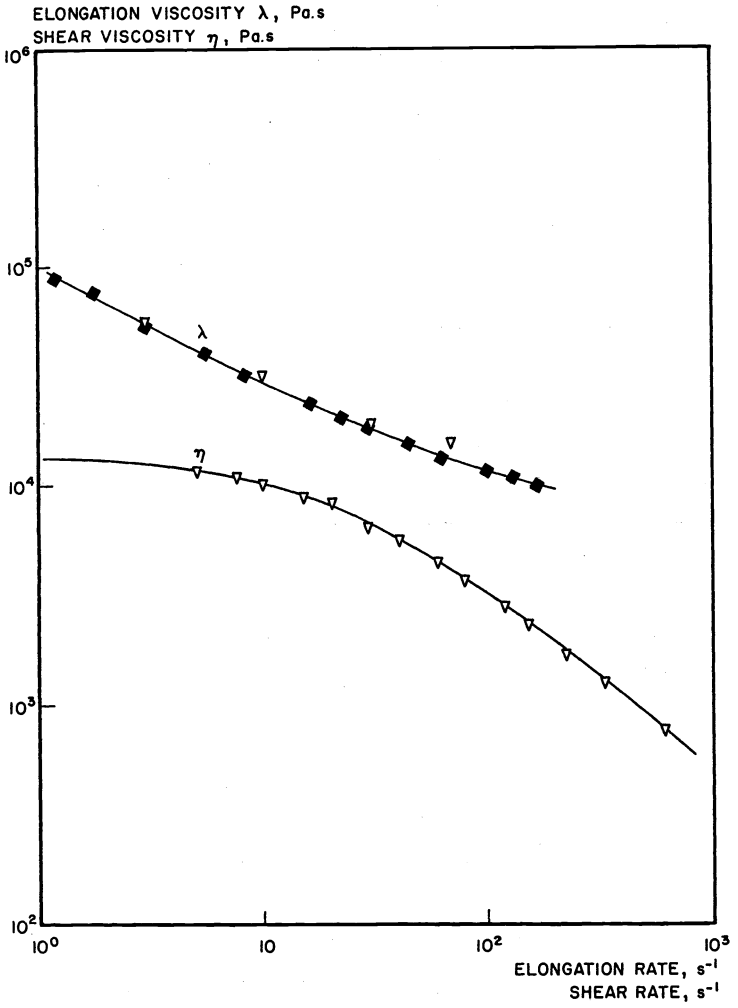

Fig. 24. Elongation viscosity data at 150 °C. Shear viscosity data are included for comparison

9. ELONGATION FLOW

Converging flow studies

Lab. F and Lab. J have performed converging flow studies at a temperature of 150 °C. From the results obtained, the elongation viscosity λ was calculated according to the procedure described by Cogswell (Ref. 16).

Fig. 24 shows the results plotted as elongation viscosity as a function of elongation rate. Fig. 24 also contains the shear viscosity data of Lab. F. From Fig. 24 it follows that the elongation viscosity is tension thinning in the stress region 10^5 to 10^6 Pa.

It was also observed by Lab. F that slowly stretching of an extrudate at 150° leads to "necking". This type of failure is typical of tension thinning polymer melts.

10. STRUCTURAL CHANGES DURING FLOW

Using quite different techniques, several laboratories have obtained information about changes in morphology occurring during the flow. Lab. N has measured the flow birefringence in a slit capillary at 110 °C and 130 °C. They found that the birefringence, $n_{11}-n_{33}$, independent of the temperature shows a negative increment with increasing shear stress until a shear stress of 4×10^5 Pa where the birefringence starts to fluctuate and becomes independent of shear stress. Also the extruded strands were birefringent. From these results it can be concluded that the birefringence increase is almost entirely due to the orientation of the polystyrene component of the polymer (see also ref. 17). Some of the extrudates were also studied by small-angle X-ray scattering (SAXS). The SAXS data indicate that the strips extruded at 0.6 and 60 s^{-1} consist of hexagonally packed polystyrene cylinders embedded in a polybutadiene matrix. Similar orientation effects of the polystyrene cylinders were found by Lab. D in quenched extrudates ($\dot{\gamma}$ = 7.5 s^{-1} at 150 °C) using electron miscroscopy.

Lab. F has carried out a number of tensile experiments on highly oriented injection moulded samples. It was found that the samples have quite different stiffnesses in the directions parallel to and perpendicular to the flow direction not only at room temperature but also at a temperature of 160 °C.

11. DISCUSSION

The observed deviation of the rheological behaviour of CARIFLEX TR-1102 from that of the pure homopolymers of the same molecular weight and molecular weight distribution can largely be explained in terms of the domain structure which persists into the melt.

Figure 25 shows the resulting viscosity-shear rate relation of CARIFLEX TR-1102 at 150 °C

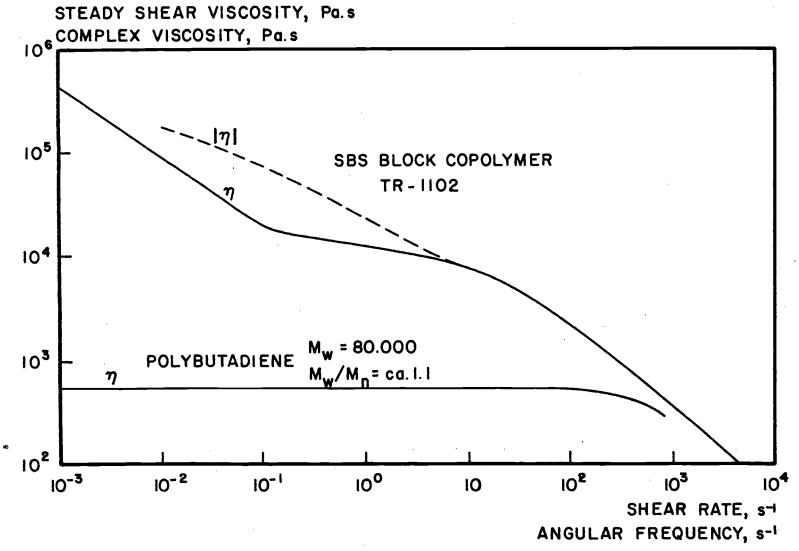

Fig. 25. Viscosity data of CARIFLEX TR-1102 and polybutadiene at 150 °C

obtained by capillary and cone and plate measurements in steady shear in comparison with the viscosity function of a polybutadiene of the same molecular weight and molecular weight distribution. Also the complex viscosity data of CARIFLEX TR-1102 at 150 °C are included. From Fig. 25 it follows that, unlike the flow curve of polybutadiene, the steady-shear flow curve of the SBS block copolymer consists of three different parts as predicted on theoretical considerations by Arnold and Meier (Ref. 3).

The response at low shear rate is that of a three dimensional network of which the crosslinks are formed by the polystyrene domains. In these domains, flow of polystyrene segments is possible, the more so at higher shear stresses where the segments can even be pulled out of the domains. As a result of this network breakdown, the viscosity strongly decreases with increasing shear rate* in that region. A similar flow behaviour at low shear rates has also been observed for ethylene-propylene copolymers (Ref. 18) and acrylonitrile-butadiene-styrene (ABS) copolymers (Ref. 19). At shear stresses higher than ca. 3000 Pa ($\dot{\gamma}$ = ca. 0.1 s^{-1}), the viscosity no longer strongly depends upon shear rate, which indicates almost complete disruption of the network. At a shear stress of 3000 Pa even the shape of the shear stress-time traces changes (see Figure 9). Below this stress level, a pronounced maximum is present followed by a continuous decrease of the shear stress caused by the time-dependent disrupture of the network. At higher shear stresses this maximum disappears and the shear stress reaches its equilibrium within a rather short time. A similar behaviour is observed in the normal stress measurements (see section 5.3). Up to shear rates of 10 s^{-1}, however, domains are still found to be present, as follows from electron microscopy data on quenched extrudates of Lab. D which show a highly oriented domain structure and from the temperature dependence of the viscosity (section 4.1.3). This implies the existence of star-shaped branched aggregates with high functionality. The observed viscosity behaviour at intermediate shear rates ($0.1 < \dot{\gamma} < 10$ s^{-1}) is thought to be the response of such a "star" structure. A similar behaviour, in fact, has been reported for several star-shaped branched and also randomly branched polymers (see, e.g., reference 20).

At very high shear rates (shear stresses), more and more polystyrene segments will be removed from the domains, ultimately resulting in a state consisting of individual molecules no longer linked together by domains. It can not be concluded from the available data where this transition actually occurs.

The complex viscosity versus frequency curves exhibit a somewhat different behaviour. First of all, it is evident from Fig. 25 that in the low shear region the complex viscosities are considerably higher than the steady-shear viscosities at equal values of $\dot{\gamma}$ and ω. Both viscosity curves come together at an ω value of about 5 s^{-1}, at which frequency also the dynamic viscosity η' and the loss factor tan δ show a pronounced transition (see Fig. 20). The frequency value of 5 s^{-1} corresponds with a shear stress of 3 x 10^3 Pa above which level, according to the steady-shear experiments, the network is assumed to be completely disrupted. This implies that above a frequency of 5 s^{-1} the melt mainly consists of star-shaped branched aggregates, for which class of materials the empirical Cox and Merz relation is found to be valid. At lower frequencies (< 5 s^{-1}) a network is present, the disrupture of which is shear stress dependent. As at equal values of $\dot{\gamma}$ and ω the shear stresses involved in the steady-shear experiments were higher than in the dynamic experiments, the amount of network breakdown was higher in the steady-shear experiments thus resulting in much lower viscosities. Dynamic experiments performed at amplitudes higher than 0.2, corresponding with shear stresses higher than again 3 x 10^3 Pa, resulted in complex viscosity values much more close to the steady-shear viscosities.

The fact that the network structure, and hence also the viscosity, is very sensitive to the application of both steady and oscillatory shear, explains that the rheological data in the low shear region are very poorly reproducible. Small differences in network structure introduced during preparation and/or testing can already lead to e.g. considerable viscosity differences (cf. sections 5.1.1 and 7). Previous shearing at a relatively high shear rate as in the special experiments of Lab. I and Lab. L (see Fig. 21) can even completely destroy the network structure, so that the viscosity response measured at low shear rates is that of a "star" structure of which the viscosity can be a factor 20 or more lower.

From these special experiments it can also be concluded that the disrupted network restores itself slowly during rest - a process which is accompanied by considerable viscosity increases.

---

* A low or high shear rate involves also a low or high shear stress, which latter is thought to be the governing factor for the breakdown of the domains

Also the data on shear stress relaxation can be interpreted in terms of the domain structure. The most striking result is the existence of a residual shear stress P_{12}^{∞} after the cessation of shear and its dependence upon the previous shear conditions. It was found that P_{12}^{∞} was very small at very short times of previous shear deformation but increased with increasing time of deformation. This suggests that all residual stress is developed during the shear process and that the unsheared polymer does not exhibit a "yield stress". This is confirmed by the results of creep measurements which show that viscous flow occurs at shear stresses even below 10 Pa (see Fig. 23). As during the shear process the network structure is broken down and a star-shaped branched structure is formed it is assumed that the residual shear stress is caused by this star structure. As shown before, the network is completely disrupted at a shear stress of about 3×10^3 Pa so that it is expected that P_{12}^{∞} reaches its maximum when this shear stress level is exceeded in the previous shear. Unfortunately, not enough data are available but from Fig. 15 it follows that P_{12}^{∞} reaches a value of 350 Pa for P_{12} = ca. 3000 Pa whereas the P_{12}^{∞} values measured by Lab. A are about 200 Pa for P_{12} values well below 3000 Pa (see e.g. Fig. 18).

Another possible consequence of the domain structure is the somewhat lower die swell of TR-1102 at shear stresses below 10^5 Pa compared to homopolymers of the same molecular weight and molecular weight distribution. At shear stresses above 10^3 Pa the domain structure is still present, namely in the form of the "star" structure (see Fig. 25). These star aggregates hardly deform during flow and thus can be considered to act as a filler, which is known to lower the die swell of polymers. The independence of extrudate swell (and also birefringence) of temperature is not only characteristic of block copolymers, but has also been observed e.g. for polystyrenes. The normal stress data follow the same trend as the extrudate swell data. At low shear stresses very low values for the normal stress were found (sometimes even negative values!, Ref. 21) whereas at higher shear stresses the normal stress values were relatively high. The negative values found at low shear stresses may be due to the effect of small volume changes on the measured thrust.

12. CONCLUSIONS

The rheological behaviour of CARIFLEX TR-1102 exhibits a number of unusual characteristics when compared with that of random copolymers of the same composition and molecular weight, viz.

(i) the melt viscosity of the block copolymer is much higher than that of otherwise similar random copolymers, especially at low shear rates;

(ii) no constant viscosity is found even at shear rates as low as 10^{-5} s^{-1};

(iii) the viscosity at low shear rates is very sensitive to shear history; this results in a large scatter in the experimental data, both of, and between, the various participants;

(iv) in the low shear region (shear stresses < 3000 Pa) the complex viscosity is as much as three times the steady-shear viscosity at equal values of frequency and shear rate; this implies that the empirical relation of Cox and Merz is not valid for the block copolymer;

(v) a residual shear stress is observed in shear stress relaxation experiments; this residual stress is developed during the shear process and its value depends upon the previous shear conditions.

The observed rheological behaviour of CARIFLEX TR-1102 can be largely explained in terms of structural changes taking place in the melt. The rheological response under low shear conditions can be explained by assuming the existence of a network structure which is broken down by shear forces. The results indicate that the network is completely disrupted at shear stresses above about 3000 Pa, which value can then be considered as a measure of the "shear strength" of the network. Evidence also exists that at shear stresses higher than 3000 Pa discrete domains are still present, but that they now form the branch points of a star-shaped branched structure. The observed rheological behaviour in the high shear region is in agreement with the presence of such a star structure. The disruption of the network structure and the concomitant formation of a star structure is thought to be responsible for the development of a residual shear stress in stress relaxation experiments.

13. RECOMMENDATIONS FOR FUTURE WORK

Possibilities for future rheological work on CARIFLEX TR-1102 are in our opinion:

- to perform additional dynamic experiments in order to verify the value of the proposed network strength;
- to perform additional experiments at temperatures other than 150 °C to investigate the temperature dependence of the strength of the network and of the residual shear stress.

Future work could also include other block copolymers:

- As the effect of styrene block length and that of total molecular weight is expected to influence the domain structure and hence the rheological properties, examination of SBS block copolymers with different composition could be of further interest.
- For comparison purposes, it would also be useful to include a block copolymer of the SB type in which star-shaped aggregates are present but no longer linked together into a network.

REFERENCES

1. G. Kraus and J.T. Gruver, J. Appl. Polymer Sci., 11, 2121 (1967).
2. G. Holden, E.T. Bishop and N.R. Legge, J. Polymer Sci.C., 26, 37 (1969).
3. K.R. Arnold and D.J. Meier, J. Appl. Polymer Sci., 14, 427 (1970).
4. D.J. Meier, J. Polymer Sci.C., 26, 81 (1969).
5. H.J.M.A. Mieras and E.A. Wilson, J. of the IRI, 7, 72 (1973).
6. J. Duglosz, A. Keller and E. Pedemonte, Kolloid-Z.u.Z. Polymere, 242, 1125 (1970).
7. F.N. Cogswell, Plastics and Polymers, 41,39 (1973).
8. J.L.S. Wales, J. Polymer Sci.C., 50, 469 (1975).
9. J.T. Gruver and G. Kraus, J. Polymer Sci. A, 2, 797 (1964).
10. G.H. West, R.N. Haward and B. Wright, SCI Monograph no. 26, 348 (1967).
11. G. Kraus and J.T. Gruver, Trans. Soc. Rheol., 13, 315 (1969).
12. W.W. Graessley, A.D. Glasscock and R.L. Crawdley, Trans. Soc. Rheol. 14, 519 (1970).
13. C.I. Chung and J.C. Gale, J. Polymer Sci.,Polym. Phys. Ed., 14, 1149 (1976).
14. W.P. Cox and E.H. Merz, J. Polymer Sci., 28, 619 (1958).
15. G. Kraus, F.E. Naylor and K.W. Rollman, J. Polymer Sci., A-2, 9, 1839 (1971).
16. F.N. Cogswell, Rheol. Acta, 9, 187 (1969).
17. M.J. Folkes and A. Keller, Polymer, 12, 222 (1971).
18. F.N. Cogswell and D.E. Hansen, Polymer, 16, 936 (1975).
19. H. Münstedt, Proc. VIIth Int. Congr. Rheology 1976, 6, 496.
20. A. Ghijsels and H.J.M.A. Mieras, J. Polymer Sci.,Polym. Phys. Ed., 11, 1849 (1973).
21. T.A. Huang, Dissertation Abstracts, 37, Ser. B, 5741 (1976).